European Journal of Mechanics B/Fluids 28 (2009) 321–327

Contents lists available at ScienceDirect

European Journal of Mechanics B/Fluids

www.elsevier.com/locate/ejmflu

Darcy–Brinkman flow past a two-dimensional screen

C.Y. Wang

Department of Mathematics, Michigan State University, East Lansing, MI 48824, USA

ARTICLE INFO

Article history:
Received 10 April 2008
Received in revised form 8 August 2008
Accepted 22 August 2008
Available online 30 August 2008

Keywords:
Flow
Porous
Darcy–Brinkman
Screen
Resistance

ABSTRACT

The flow past a screen composed of periodic slats in a plane is studied. The method of eigenfunction expansions and point match is used to solve the Darcy–Brinkman equations. The velocities, pressures and resistances are determined for the flow in three orthogonal directions. Aside from screen geometry, the flow is governed by a porous media parameter k which is zero for pure viscous flow. The fundamental case for the flow over a single slat is then extrapolated. It is found that for $k = 0$ the Stokes paradox occurs and the drag rises singularly as k is increased from zero.

1. Introduction

The flow past a screen is important in biological membrane and industrial filtering processes. Due to the small velocity in the crevices, the inertial effects can be ignored and creeping flow assumptions are valid. Analytical solutions are difficult for viscous flow even in the Stokes limit. For thin screens with negligible thickness, Roscoe [1] used an electrostatic potential method to solve for the Stokes flow through an elliptic hole. Roscoe's transform was applied to the slow viscous flow through periodic two-dimensional slits by Hasimoto [2], who was able to express the solution in closed form. Wang [3] used the Roscoe transform semi-analytically for the solution to viscous flow through an array of holes.

In this paper we are concerned with the flow past a thin screen embedded in a porous medium. We shall see later that there are some fundamental differences between Darcy–Brinkman flow and Stokes flow.

The flow in a porous medium is traditionally approximated by the Darcy equation, where the mean velocity is proportional to the pressure gradient, resulting in potential flow. Brinkman added a viscous term so that the no slip condition on solid surfaces can be applied. The Darcy–Brinkman equation is [4–6]

$$\nabla p' = \mu_e \nabla^2 \vec{v} - \frac{\mu}{K}\vec{v} \tag{1}$$

where p' is the pressure, μ_e is the effective viscosity of the matrix, $\vec{v}$ is the velocity vector, μ is the viscosity of the fluid, and K is the permeability. This equation is well accepted for porous media of high porosity such as fiberglass wool. The Darcy–Brinkman equation reduces to Darcy equation when $K \to 0$ and to the Stokes equation when $K \to \infty$. In both limits the problem can be simplified by a velocity potential.

However, for the general Darcy–Brinkman equation, all potential methods fail. We shall use semi-analytic eigenfunction expansions and point match to solve the problem.

Since Eq. (1) is linear, any uniform flow towards a screen can be separated into three independent flows: the flow normal to a screen (Fig. 1(a)), the flow parallel to a screen but still normal to the slats (Fig. 1(b)) and the parallel flow parallel to the slats (Fig. 1(c)). In each case the flow is two dimensional, i.e. depends on x, y directions only. Note that if the Darcy equation is used in the last two cases, the screen would have no effect on the flow.

2. The flow normal to the screen

The top of Fig. 1(a) shows the two-dimensional thin screen. The width of the slats is $2L$ and the period is $2bL$. Cartesian axes are placed at the middle of a slat as shown. We normalize all lengths by L, velocities by the velocity at infinity U, the pressure by $\mu_e U/L$. For the flow normal to the screen, the normalized cross section is shown at the bottom of Fig. 1(a). Define a stream function ψ normalized by UL which satisfies continuity, where the Cartesian velocity components are $(\psi_y, -\psi_x)$. Eq. (1) then becomes

$$p_x = \nabla^2 \psi_y - k^2 \psi_y, \tag{2}$$

$$p_y = -\nabla^2 \psi_x + k^2 \psi_x \tag{3}$$

where

$$k^2 = \frac{\mu L^2}{\mu_e K} \tag{4}$$

E-mail address: cywang@mth.msu.edu.

0997-7546/$ – see front matter
doi:10.1016/j.euromechflu.2008.08.003

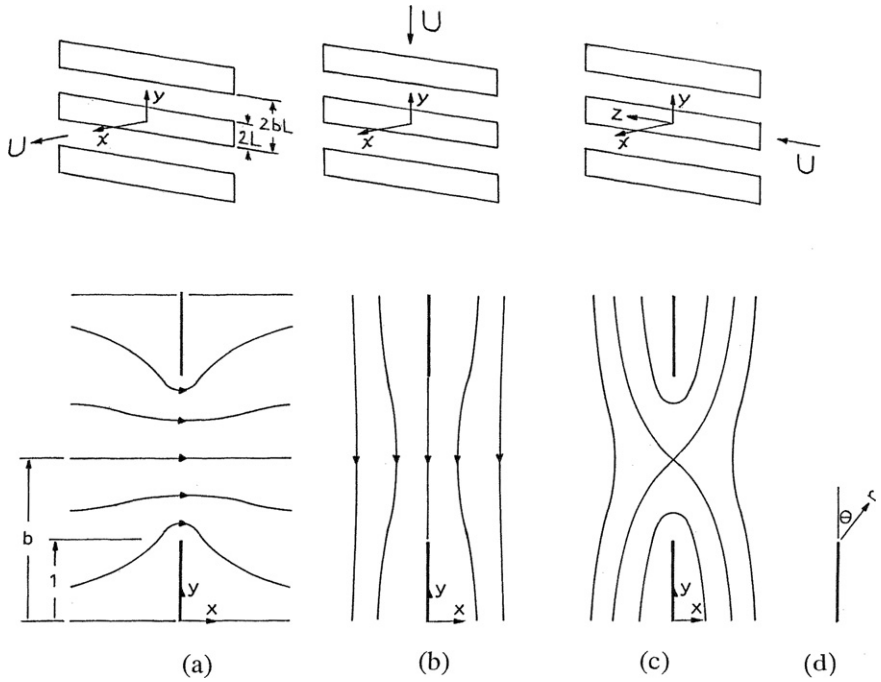

Fig. 1. The top figures show the three orthogonal flow directions across the screen. The bottom figures are the cross sections of each case. (a) The flow is normal to the screen. The mean flow is in the x direction. Some streamlines are shown in the cross section. (b) The flow is parallel to the screen, but normal to the slats. The mean flow is in the $-y$ direction. Streamlines are shown. (c) Parallel flow is parallel to the slats. The flow is in the z direction. Constant velocity lines are shown. (d) Coordinates in the vicinity of an edge.

is an important non-dimensional parameter characterizing the porous medium. Eliminating pressure from Eqs. (2), (3) yields

$$\nabla^2\left(\nabla^2 - k^2\right)\psi = 0. \tag{5}$$

Due to symmetry, we need to consider only the strip $x \geqslant 0$, $0 \leqslant y \leqslant b$ which is our computational domain. The symmetry boundary conditions are

$$\psi = 0, \quad \psi_{yy} = 0 \quad \text{on } y = 0, \tag{6}$$

$$\psi = b, \quad \psi_{yy} = 0 \quad \text{on } y = b, \tag{7}$$

$$\psi_x = 0, \quad \psi_{xxx} = 0 \quad \text{on } x = 0,\ 1 < y \leqslant b. \tag{8a,b}$$

The no-slip boundary condition is

$$\psi_x = 0, \quad \psi = 0 \quad \text{on } x = 0,\ 0 \leqslant y < 1. \tag{9a,b}$$

At infinity the flow is uniform, such that $\psi_y = 1$. The solution to Eqs. (5)–(7), (8a), (9a) is

$$\psi = y + \sum_{n=1}^{\infty} A_n \sin(\alpha_n y)\left(e^{-\alpha_n x} - \frac{\alpha_n}{\sqrt{\alpha_n^2 + k^2}} e^{-\sqrt{\alpha_n^2 + k^2}\,x}\right) \tag{10}$$

where $\alpha_n = n\pi/b$ and A_n are coefficients to be determined. The remaining boundary conditions are satisfied by point match. Truncate the series to N terms and consider N equally-spaced points $y_j = b(j - .5)/N$, $j = 1, \ldots, N$. Then Eq. (8b) becomes

$$\sum_{n=1}^{N} A_n \sin(\alpha_n y_j)\alpha_n = 0, \quad 1 < y_j \leqslant b. \tag{11}$$

Eq. (9b) yields

$$\sum_{n=1}^{N} A_n \sin(\alpha_n y_j)\left(1 - \frac{\alpha_n}{\sqrt{\alpha_n^2 + k^2}}\right) = -y_j, \quad 0 \leqslant y_j < 1. \tag{12}$$

From Eqs. (11), (12) the coefficients A_n are inverted. Convergence is fairly fast. In general $N = 100$ is adequate for a three figure accuracy in ψ. From Eqs. (2), (3) pressure is integrated to be

$$p = -k^2 x + k^2 \sum_{1}^{N} A_n \cos(\alpha_n y) e^{-\alpha_n x} + c. \tag{13}$$

The integration constant c is determined by setting the average pressure at $x = 0$, $1 < y \leqslant b$ to zero. Thus

$$c = \frac{k^2}{b-1} \sum_{1}^{N} A_n \frac{\sin\alpha_n}{\alpha_n}. \tag{14}$$

Typical streamlines are shown in Fig. 2(a) and the corresponding pressure distribution is shown in Fig. 2(b). Note the convergence of the pressure lines at the edge of the slat. Such singularity in pressure is analyzed in Section 5. The value $\Delta p = |2c|$ also represents the additional pressure loss due to the screen. Fig. 3 shows for given spacing b, Δp rises with the porous parameter k. When $k \to 0$, the pressure drop approaches that predicted by Hasimoto [2]

$$\Delta p = \frac{2\pi/b}{|\ln[\cos((b-1)\pi/2b)]|}. \tag{15}$$

Our computed numerical values from Eq. (14) agrees with those of Eq. (15) as $k \to 0$.

Of interest is the force on a single slat, which can be isolated by increasing the distance b. Both consideration of momentum difference and integration of pressure difference on a single slat shows the (drag) force is $D = 2b\Delta p$. Since it is not possible to use $b = \infty$ in our computation, the single slat or plate problem is approached as follows. Assuming for large b

$$D \sim a_0 + a_1/b^2 + \cdots. \tag{16}$$

For given k we compute D for large b using an N which guarantees at least 10 collocation points on the slat (up to $N = 2000$). Then D is plotted against $1/b^2$ for various b. A typical result is shown

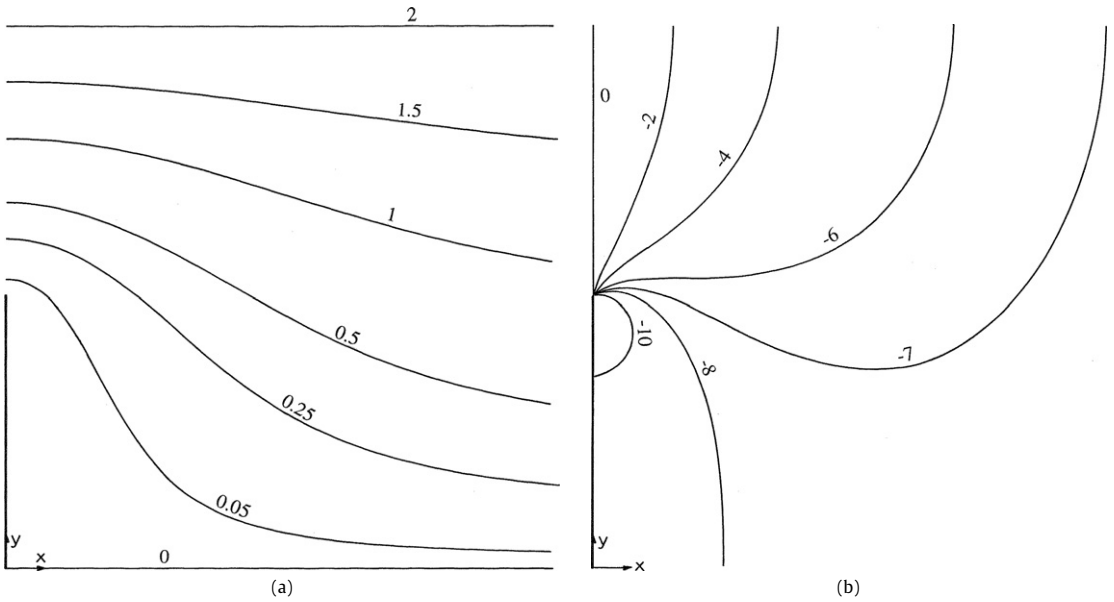

Fig. 2. (a) Typical streamlines for flow normal to screen (see Fig. 1(a)). $b = 2$, $k = 1$. (b) The corresponding pressure distribution. The thick line at the left side is half of a slat, with normalized length of one. The computational domain is $x \geqslant 0$, $0 \leqslant y \leqslant b = 2$. Only 1/4 of a period is shown.

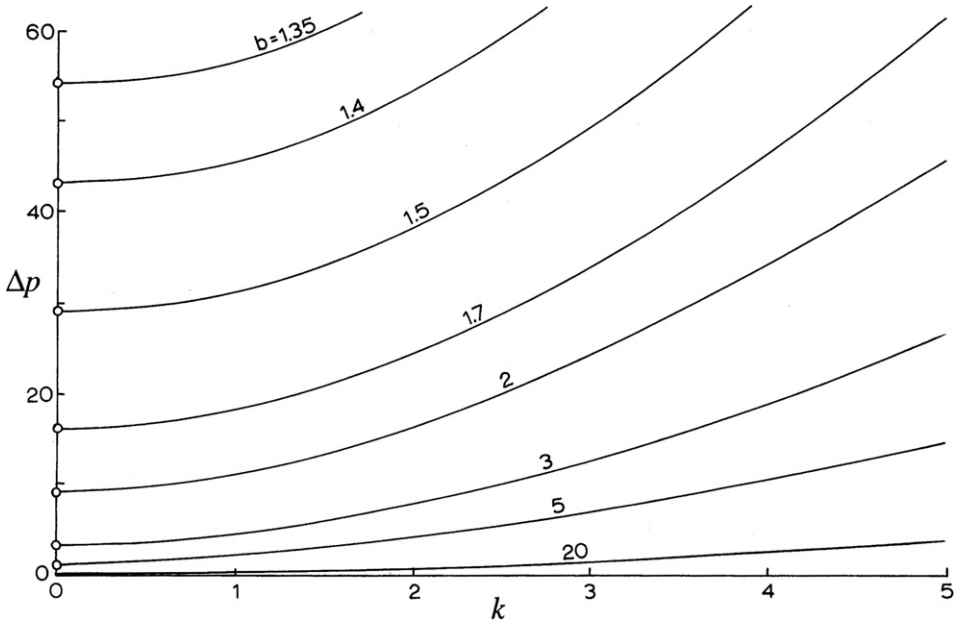

Fig. 3. The additional pressure loss due to the screen. Circles are Stokes flow results from Eq. (15) or [2].

Table 1
Drag due to flow normal to a single slat

k	0	0.1	0.2	0.5	1	2	3.5	5
D	0	5.15	6.60	11.0	19.5	41.3	86.2	146.

in the inset of Fig. 4 for $k = 1$. The values for drag from $b = 6$ to $b = 20$ seem to lie in a straight line, which gives credence to the form of Eq. (16). Extrapolation to $b \to \infty$ yields $D = 19.52$ for a single slat. Similarly, the drag for other k values are obtained, and plotted in Fig. 4. Since the drag on a single slat is fundamental, some numerical values are given in Table 1.

The drag is zero for $k = 0$ or Stokes flow, which can also be seen from Eq. (15). The singular rise with k is similar to the drag of a circular cylinder, for which Stokes flow does not exist (see Appendix A on the Stokes paradox).

3. The flow parallel to the screen and normal to the slats

Fig. 1(b) shows uniform flow parallel to the plane of the screen. The governing equation is still Eq. (5). At large x we need $\psi_x = 1$ and the other boundary conditions are

$$\psi_y = 0, \quad \psi_{yyy} = 0 \quad \text{on } y = 0, \tag{17}$$

$$\psi_y = 0, \quad \psi_{yyy} = 0 \quad \text{on } y = b, \tag{18}$$

$$\psi = 0, \quad \psi_{xx} = 0 \quad \text{on } x = 0, \ 1 < y \leqslant b, \tag{19a,b}$$

$$\psi = 0, \quad \psi_x = 0 \quad \text{on } x = 0, \ 0 \leqslant y < 1. \tag{20a,b}$$

The solution to Eqs. (5), (17), (18), (19a), (20a) is

$$\psi = x + \sum_{n=0}^{\infty} B_n \cos(\alpha_n y)\left(e^{-\alpha_n x} - e^{-\sqrt{\alpha_n^2 + k^2}\,x}\right) \tag{21}$$

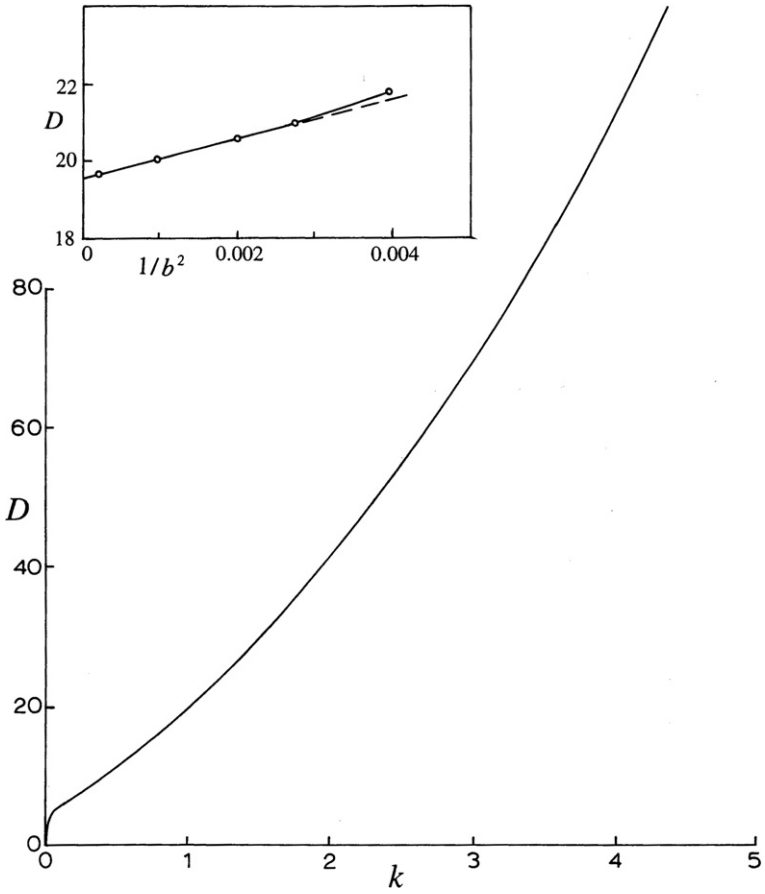

Fig. 4. Drag force due to normal flow on a single slat. Note singular rise near $k = 0$. The inset shows typical extrapolation to $b \to \infty$ for $k = 1$. Form right, the small circles are $b = 5, 6, 7, 10, 20$.

Eqs. (19b), (20b) then yield the collocation conditions

$$\sum_{n=0}^{N-1} B_n \cos(\alpha_n y_j) = 0, \quad 1 < y_j \leqslant b, \tag{22}$$

$$\sum_{n=0}^{N-1} B_n \cos(\alpha_n y_j)\left(\alpha_n - \sqrt{\alpha_n^2 + k^2}\right) = 1, \quad 0 \leqslant y_j < 1. \tag{23}$$

The coefficients B_n are inverted as before. The pressure is

$$p = k^2 y - k^2 \sum_{0}^{N-1} B_n \sin(\alpha_n y) e^{-\alpha_n x}. \tag{24}$$

Typical streamlines and pressure distribution are shown in Fig. 5. The force on the slat is due solely to shear stress. Using the stream function to obtain shear, we find

$$D = -k^2 \left(B_0 + \sum_{1}^{N-1} B_n \frac{\sin \alpha_n}{\alpha_n} \right). \tag{25}$$

The drag is plotted in Fig. 6. The drag rises with k, but is lower when the slats are close together, opposite to the case when the flow is normal. In fact, when there are no gaps ($b = 1$), the screen becomes a single plate with the parallel velocity distribution

$$\upsilon = -\left(1 - e^{-kx}\right). \tag{26}$$

The shear drag for a segment of length 2 is thus $D = 4k$. The drag is zero when $k = 0$, confirming the Stokes paradox for the steady parallel flow over an infinite plate. The drag for a single slat is extrapolated from $b \to \infty$ values. Table 2 shows some numerical values.

Table 2
Drag due to flow parallel but transverse to a single slat

k	0	0.1	0.2	0.5	1	2	3.5	5
D	0	3.43	4.20	6.07	8.59	13.16	19.66	26.01

4. Longitudinal parallel flow

Fig. 1(c) shows the flow is longitudinal along the slats. Let w be the velocity in the z direction, uniform at infinity, driven by a constant pressure gradient. The governing equation is

$$\left(\nabla^2 - k^2\right) w = -k^2 \tag{27}$$

where w is zero on the slats. The solution which is symmetrical at $y = 0$ and $y = b$ is

$$w = 1 + \sum_{0}^{N-1} C_n \cos(\alpha_n y) e^{-\sqrt{\alpha_n^2 + k^2}\, x}. \tag{28}$$

At $x = 0$ the boundary conditions are $w = 0$ when $0 \leqslant y < 1$, and $w_x = 0$ when $1 < y \leqslant b$, or

$$\sum_{n=0}^{N-1} C_n \sqrt{\alpha_n^2 + k^2} \cos(\alpha_n y_j) = 0, \quad 1 < y_j \leqslant b, \tag{29}$$

$$\sum_{n=0}^{N-1} C_n \cos(\alpha_n y_j) = -1, \quad 0 \leqslant y_j < 1. \tag{30}$$

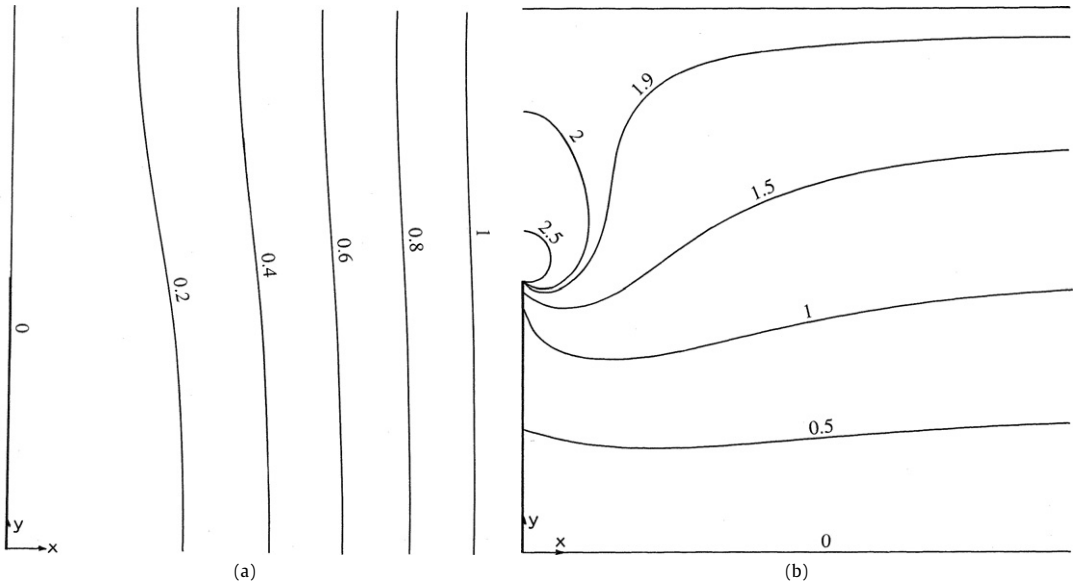

Fig. 5. (a) Typical streamlines for flow parallel to screen, but normal to the slats (see Fig. 1(b)). $b = 2$, $k = 1$. (b) The corresponding pressure distribution. Other explanations are similar to those of Fig. 2.

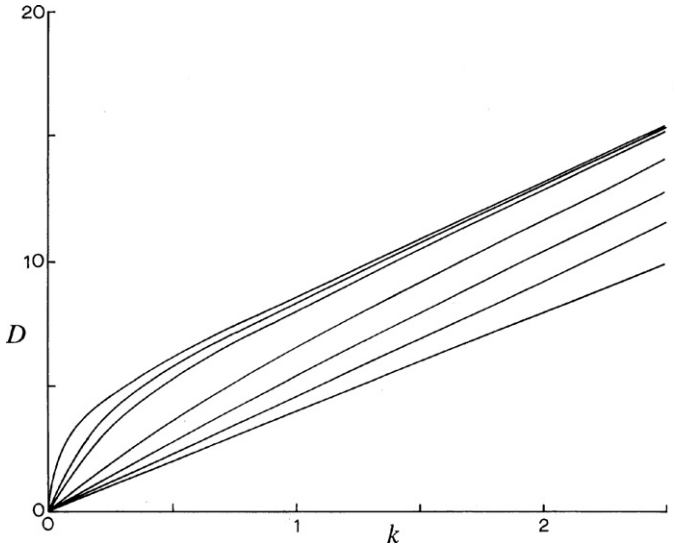

Fig. 6. Drag force per slat for flow parallel to the screen. Form bottom: $b = 1, 1.2, 1.5, 2, 10, \infty$. For a continuous plate, $b = 1$ and $D = 4k$. The $b = \infty$ curve is the force on a single slat.

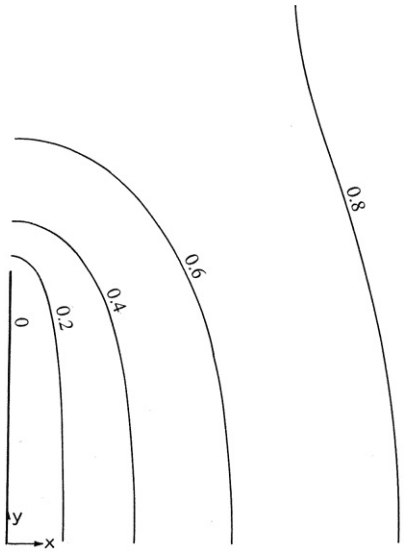

Fig. 7. Typical constant velocity lines for parallel flow parallel to the slats (see Fig. 1(c)). $b = 2$, $k = 1$. Other explanations are similar to those of Fig. 2.

Table 3
Drag due to parallel flow along a single slat

k	0	0.1	0.2	0.5	1	2	3.5	5
D	0	2.01	2.56	3.91	5.95	9.95	15.9	21.9

The coefficient C_n in Eqs. (29), (30) are solved for $j = 1, \ldots, N$. Fig. 7 shows typical constant velocity lines. The force on the slat is solely due to shear. We find

$$D = -4\left(kC_0 + \sum_{n=1}^{N-1} C_n \sqrt{\alpha_n^2 + k^2}\,\frac{\sin(\alpha_n)}{\alpha_n}\right). \tag{31}$$

The result is plotted in Fig. 8. Again when $b = 1$ (continuous plate) the drag is $D = 4k$. The extrapolated $b \to \infty$ (single slat) value shows singular rise from zero. Some values are given in Table 3.

5. Edge singularity

Consider the top edge of a slat and attach cylindrical coordinates (r, θ) as shown in Fig. 1(d). In the vicinity very close to the tip r is very small and Eq. (5) reduces to the biharmonic equation

$$\nabla^4 \psi = 0. \tag{32}$$

The general solution is (e.g. [7])

$$\psi = \begin{cases} r^\lambda\{\sin(\lambda\theta), \cos(\lambda\theta), \sin[(\lambda-2)\theta], \cos[(\lambda-2)\theta]\}, \\ \quad \lambda \neq 0, 1, 2, \\ \{1, \theta, \sin(2\theta), \cos(2\theta)\}, \quad \lambda = 0, \\ r\{\sin\theta, \cos\theta, \theta\sin\theta, \theta\cos\theta\}, \quad \lambda = 1, \\ r^2\{1, \theta, \sin(2\theta), \cos(2\theta)\}, \quad \lambda = 2. \end{cases} \tag{33}$$

For the flow normal to the screen, ψ is even in θ, thus

$$\psi = r^\lambda\{c_1\cos(\lambda\theta) + c_2\cos[(\lambda-2)\theta]\}. \tag{34}$$

Applying the no slip boundary conditions $\psi(r, \pi) = 0$ and $\psi_\theta(r, \pi) = 0$ yield either $c_1 + c_2 = 0$ and λ an integer, or $\lambda c_1 +$

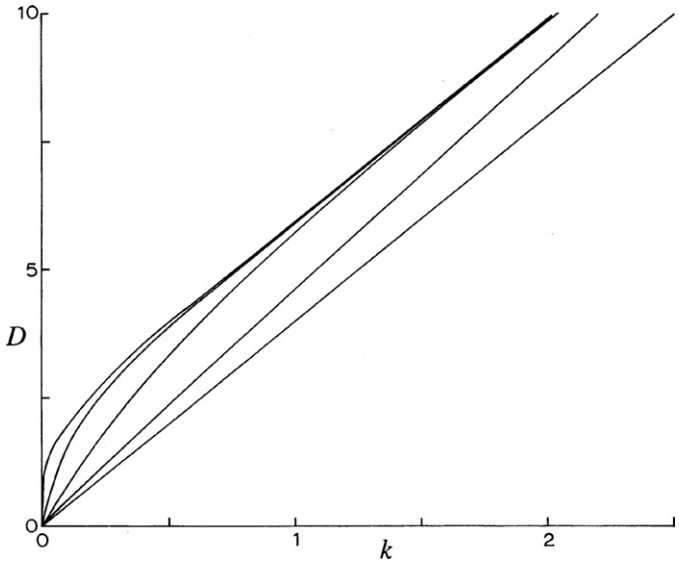

Fig. 8. Drag per slat for parallel flow parallel to the slats. Form bottom: $b = 1, 1.2, 2, 5, \infty$. For a continuous plate, $b = 1$ and $D = 4k$. The $b = \infty$ curve is the force on a single slat.

$(\lambda - 2)c_2 = 0$ and $\lambda = 1/2, 3/2, 5/2, \ldots$. Now for bounded velocity at the origin, $\lambda \geqslant 1$. If $\lambda = 1$ the solution is found to be trivial. Thus the lowest (most important) power is $\lambda = 3/2$. The dominant term is then

$$\psi \sim r^{3/2}\big[\cos(3\theta/2) + 3\cos(\theta/2)\big]. \tag{35}$$

The velocity is then proportional to $r^{1/2}$ which is bounded. The pressure, being proportional to $r^{-1/2}$, has a weak singularity. The drag or the integral of pressure, proportional to $r^{1/2}$ is non-singular.

Next consider the flow parallel to the screen and normal to the slats as in Fig. 1(b). In this case ψ is odd in θ

$$\psi = r^{\lambda}\big\{c_1 \sin(\lambda\theta) + c_2 \sin\big[(\lambda - 2)\theta\big]\big\}. \tag{36}$$

Applying the no slip conditions yield either $\lambda c_1 + (\lambda - 2)c_2 = 0$ and λ an integer, or $c_1 + c_2 = 0$ and $\lambda = 1/2, 3/2, 5/2, \ldots$. Again we find the lowest power is $\lambda = 3/2$ and

$$\psi \sim r^{3/2}\big[\sin(3\theta/2) + \sin(\theta/2)\big]. \tag{37}$$

The singular nature is similar to the previous case.

For parallel flow parallel to the slats, in the vicinity of the origin, Eq. (27) becomes the harmonic

$$\nabla^2 w = 0. \tag{38}$$

The even solution is

$$w = c_1 r^{\lambda} \cos(\lambda\theta). \tag{39}$$

The boundary condition $w(r, \pi) = 0$ yields $\lambda = 1/2, 3/2, 5/2, \ldots$. Since for bounded velocity $\lambda \geqslant 0$ the dominant term is

$$w \sim r^{1/2} \cos(\theta/2). \tag{40}$$

Only the shear stress has a $r^{-1/2}$ singularity. The shear drag is bounded.

We conclude edge singularities have little effect on our computation of flow and drag force.

6. Discussions and conclusion

The flow through a porous medium is governed by the important parameter k. It is close to the inverse square root of the Darcy number. For materials such as sand or gravel, k could be very large, while for materials with high porosity (for which the Darcy–Brinkman equations is more suitable), k could be as low as 0.001 (e.g. fiberglass wool).

Unlike the Stokes equation, the Darcy–Brinkman equation is not amenable to the Roscoe transform or complex transforms. Our method of eigenfunction expansions is efficient except when b is close to one or very large.

For the same screen geometry, the resistance is highest for the flow normal to the screen, and lowest for the parallel flow along the slat direction. When the gap between the slats diminish ($b \to 1$) the resistance becomes infinite for the flow normal to the screen, while in the other two directions the drag per slat is $4k$.

The drag force on a single slat is of fundamental importance, and determined here for the first time. As in the case of the flow over a circular cylinder (Appendix A), the Stokes paradox (non-existence of a solution) occurs for the single slat when $k = 0$. From the circular cylinder results one may infer the following for all cylinders, including the single slat. The drag is zero for $k = 0$ and increases singularly from zero as $1/|\ln k|$. For large k, the drag due to the flow across a cylinder is proportional to k^2 for large k, while in the other two orthogonal directions the drag is proportional to k.

Appendix A. Stokes paradox

The non-existence for Stokes flow over a two dimensional cylinder (Stokes paradox) is well known. We study whether the Stoke paradox persists for Darcy–Brinkman flow, which in the limit of $k \to 0$ is Stokes flow. The only exact solution is for the flow over a circular cylinder. In cylindrical coordinates (r, θ) Eq. (5) has the solution

$$\psi = \sin\theta\left[r - \left(1 + \frac{2K_1(k)}{kK_0(k)}\right)\frac{1}{r} + \frac{2}{kK_0(k)}K_1(kr)\right]. \tag{A.1}$$

The stream function gives uniform flow at infinity, and no slip on the cylinder at $r = 1$. This solution becomes zero as $k \to 0$, confirming the Stokes paradox. However, the flow exists for k small but non-zero. The pressure is integrated to be

$$p = p_0 - k^2 \cos\theta\left[r + \left(1 + \frac{2K_1(k)}{kK_0(k)}\right)\frac{1}{r}\right]. \tag{A.2}$$

The pressure drag is

$$D_p = 2\pi k^2\left(1 + \frac{K_1(k)}{kK_0(k)}\right). \tag{A.3}$$

The shear drag is

$$D_s = 2\pi\frac{kK_1(k)}{K_0(k)}. \tag{A.4}$$

The total force on the cylinder is thus

$$D = 2\pi\left(k^2 + \frac{2kK_1(k)}{K_0(k)}\right). \tag{A.5}$$

Expanding the Bessel functions [8] we find for large k, the force is asymptotically

$$D \sim 2\pi k^2 + 4\pi k + \cdots \tag{A.6}$$

while for small k

$$D \sim \frac{4\pi}{|\ln k|} + \cdots \tag{A.7}$$

which rises singularly as k is increased from zero. We expect similar singular behavior exists for the Darcy–Brinkman flow over a single plate as well.

For longitudinal flow along a cylinder, Eq. (27) gives

$$w = 1 - \frac{K_0(kr)}{K_0(k)}. \tag{A.8}$$

The drag is due solely to shear

$$D = 2\pi \frac{kK_1(k)}{K_0(k)}. \tag{A.9}$$

For large k

$$D \sim 2\pi k + \mathrm{O}(1). \tag{A.10}$$

As $k \to 0$ we find

$$D \sim \frac{2\pi}{|\ln k|} + \cdots \tag{A.11}$$

which also rises singularly from zero.

References

[1] R. Roscoe, The flow of viscous fluids round plane obstacles, Philos. Mag. 40 (1949) 338–351.
[2] H. Hasimoto, On the flow of a viscous fluid past a thin screen at small Reynolds numbers, J. Phys. Soc. Jpn. 13 (1958) 632–639.
[3] C.Y. Wang, Stokes flow through a thin screen with patterned holes, AIChE J. 40 (1994) 419–423.
[4] H.C. Brinkman, A calculation of the viscous force exerted by a flowing fluid in a dense swarm of particles, Appl. Sci. Res. A 1 (1947) 27–34.
[5] I.D. Howells, Drag due to the motion of a Newtonian fluid through a sparse random array of fixed rigid objects, J. Fluid Mech. 64 (1974) 449–475.
[6] D.B. Ingham, I. Pop, Transport in Porous Media, Pergamon, Oxford, 2002.
[7] F.S. Sherman, Viscous Flow, McGraw-Hill, New York, 1990.
[8] M. Abramowitz, I.A. Stegun, Handbook of Mathematical Functions, Dover, New York, 1965.